Numerical modeling of acoustic instability in a nonequilibrium vibrationally excited gas

© S.S. Khrapov, G.S. Ivanchenko, V.P. Radchenko, A.V. Titov

Volgograd State University,
400062 Volgograd, Russia
e-mail: khrapov@volsu.ru

Based on gas-dynamic methods, numerical modeling of the nonlinear dynamics of sound waves in a vibrationally excited nonequilibrium gas was carried out and the main stages of the evolution of acoustic instability were studied. It is shown that in numerical models the linear regime with an exponential growth law of the amplitude of disturbances is in good agreement with the linear analysis of stability, and at the nonlinear stage of development of acoustic instability, a system of shock waves is formed. The effects of nonlinear saturation of the intensity of shock waves, caused by the stabilization of acoustic instability, are demonstrated.

Keywords: nonequilibrium gas, vibrational relaxation, acoustic instability, numerical modeling, CSPH-TVD method.

Introduction

The properties of nonequilibrium media are important for understanding the physical processes occurring, for example, in an oscillatory-excited gas [1]. Under certain conditions, a non-equilibrium medium becomes acoustically active, i.e. the amplitude of sound waves in it increases [2–4]. Acoustic instability in a non-equilibrium vibrationally excited gas can lead to [2]: overreflection of sound waves at the interface between equilibrium and nonequilibrium media; excitation of a headwind acoustic wind; emergence of new properties of parametric interactions of sound, vortex and entropy modes; changes in the critical Reynolds number of the laminar-turbulent transition, the structure of the boundary layer, and the coefficients of aerodynamic drag; changes in the structure, velocity and stability conditions of shock waves, as well as the parameters of the flow behind the front of detonation waves.

An important tool for studying processes and phenomena in gas-plasma media, along with a physical experiment, is a computational experiment based on the solution of hydro-dynamic equations by well-tested numerical methods [5–7]. To assess the adequacy of numerical algorithms used in numerical simulation of unstable gas-dynamic flows, it is necessary to compare the obtained simulation results with linear stability analysis [8].

The aim of this paper — is to develop a numerical model (tool) for studying the nonlinear dynamics of acoustic instability in an oscillatory-excited gas with various relaxation models based on the methods of numerical gas-dynamic simulation.

1. Mathematical Model of an Excitatory Gas

In this paper, we will confine ourselves to considering the model of a one-component oscillatory excited gas with exponential Landau relaxation−Teller [2,3,9] in a one-dimensional approximation

$$\frac{\partial \mathbf{U}}{\partial t} + \frac{\partial \mathbf{F}}{\partial x} = \mathbf{G}, \tag{1}$$

where $\mathbf{U} = \{\varrho, \varrho u, \varrho \varepsilon, \varrho \varepsilon_v\}^{\mathrm{T}}$ — is a vector of conservative variables, $\varepsilon = 0.5u^2 + p/[(\gamma - 1)\varrho]$, ϱ, u and p — density, velocity, and pressure of the gas, respectively, γ — adiabatic index, ε_v — specific vibrational energy of gas molecules, $\mathbf{F} = \{\varrho u, \varrho u^2 + p, (\varrho \varepsilon + p)u, \varrho \varepsilon_v u\}^{\mathrm{T}}$ — flux density vector of the magnitude $\mathbf{U}$,

$$\mathbf{G} = \{0, \varrho g, \varrho(\varepsilon_v - \varepsilon_v^e)/\tau - \varrho \Lambda + \varrho u g, \varrho(\varepsilon_v^e - \varepsilon_v)/\tau + \varrho Q\}^{\mathrm{T}},$$

ε_v^e — equilibrium value of specific vibrational energy, τ — oscillatory relaxation time, Q and Λ — specific heating (pumping) and cooling (heat sink) capacities, respectively. The system (1) is closed by the equation of state of the ideal gas: $p = R\varrho T$, where $R = R_*/\mathcal{M}$ — gas constant, R_* — universal gas constant, $\mathcal{M}$ — molar mass of the gas.

In the two-temperature approximation, the specific vibrational energy of the gas molecules ε_v and its equilibrium value ε_v^e are functions of the vibrational T_v and thermodynamic T temperatures, respectively [3,7,10]:

$$\varepsilon_v(T_v) = \frac{R\theta_v}{\exp(\theta_v/T_v) - 1}, \quad \varepsilon_v^e \equiv \varepsilon_v(T) = \frac{R\theta_v}{\exp(\theta_v/T) - 1}, \tag{2}$$

where θ_v — characteristic oscillatory temperature of the gas. The formulas (2) are written for a single oscillatory mode.

If a polyatomic molecule has several vibrational modes, then the total vibrational energy of the gas (considering only the first energy level of each mode) can be represented as the sum [10]:

$$\varepsilon_v = \sum_\ell r_\ell \varepsilon_{v,\ell} \quad \text{and} \quad \varepsilon_v^e = \sum_\ell r_\ell \varepsilon_{v,\ell}^e,$$

where ℓ — mode number, and r_ℓ — degree of degeneracy ℓ-mode.

In gas-dynamic calculations, model Millikan's-White [7,11] is usually used for the oscillatory relaxation time, which at temperatures below 3000 K agrees well with both experimental data and the conclusions of the kinetic theory [12]. There are other more accurate models for calculating relaxation time at higher temperatures [10,13–15]. Models based on analytical approximations of experimental data [10] are also used. In general, the oscillatory relaxation time can be written as

$$\tau(\hat{p}, T) = \frac{1}{\hat{p}} \frac{\exp(a_0 + a_1 T^{-1/3} + a_2 T^{-2/3} + a_3 T^{1/3} + n \ln T)}{1 - m \exp(-\theta_\star/T)},$$

(3)

where $\hat{p} = p/p_A$ — pressure in units of atmospheric pressure ($p_A = 101\,325$ Pa), $\theta_\star$ — minimum of the characteristic temperatures of vibrational mode [15], the coefficients a_k and n are determined experimentally [10,16] or calculated using semi-empirical formulas [11,15], and the parameter m allows you to consider ($m = 1$) or not consider ($m = 0$) the correction of the kinetic theory [15].

2. Results of numerical simulation

To numerically simulate the nonlinear dynamics of unstable sound waves in a nonequilibrium vibrationally excited gas (1)−(3), we will use the CSPH-TVD (Combined Smoothed Particle Hydrodynamics−Total Variation Diminishing, [17,18]) method, which has the second order of accuracy in terms of spatial coordinate and time. We will consider the dynamics of unstable sound waves against the background of the initial stationary and homogeneous distribution of flow parameters ($f_0 = \text{const}$) of the quiescent gas ($u_0 = 0$), and we will also confine ourselves to a model with constant values of heating and cooling functions that do not depend on density and temperature. Then, from the energy balance equations in (1) for the initial state, we obtain the following relations: $Q_0 = \Lambda_0$ and $\varepsilon_v(T_{v0}) - \varepsilon_v^e(T_0) = \tau_0 Q_0$. From the last equation it is possible to determine the initial disequilibrium of the medium, i.e. to find the vibrational temperature $T_{v0} \neq T_0$, which, in the case of diatomic molecules with one vibrational mode, can be expressed as (2)

$$T_{v0} = T_0 \bar{\theta}_v \left[\ln \frac{\bar{\theta}_v \exp \bar{\theta}_v + S (\exp \bar{\theta}_v - 1)}{\bar{\theta}_v + S (\exp \bar{\theta}_v - 1)} \right]^{-1},$$

where

$$\bar{\theta}_v = \frac{\theta_v}{T_0}, \quad S = \frac{\tau_0 Q_0}{R T_0}$$

— a dimensionless parameter that characterizes the degree of nonequilibrium of the medium in [2,3,17].

Inasmuch as in this paper we are not considering a specific gas medium, but are investigating the basic regularities of the nonlinear evolution of acoustic instability depending on the parameters of the relaxation model, it makes sense to switch to dimensionless quantities in the equations (1)−(3). This will reduce the number of calibration coefficients in our numerical simulation and simplify the procedure for comparing the results of the numerical simulation with the linear stability analysis in [2,3,17]. Let us introduce the following characteristic scales of the numerical model: $l_t = \tau_0$, $l_u = c_{s0} = \sqrt{\gamma p_0 / \varrho_0}$, $l_x = c_{s0} \tau_0$, $l_T = T_0$, $l_p = p_0$, $l_\varrho = \varrho_0 / \gamma$. Further, we will use the dimensionless quantities $\bar{f} = f / l_f$, then, considering the equation of state for the relaxation time of (3), we get:

$$\bar{\tau}(\bar{\varrho}, \bar{T}) = \frac{\gamma}{\bar{\varrho}} \exp\left\{ \bar{a}_1 \bar{T}^{-1/3} + \bar{a}_2 \bar{T}^{-2/3} + \bar{a}_3 \bar{T}^{1/3} \right.$$
$$\left. + (n - 1) \ln \bar{T} \right\} \frac{1 - m \exp(-\bar{\theta}_\star)}{1 - m \exp(-\bar{\theta}_\star / \bar{T})}, \quad (4)$$

where $\bar{a}_1 = a_1 T_0^{-1/3}$, $\bar{a}_2 = a_2 T_0^{-2/3}$, $\bar{a}_3 = a_3 T_0^{1/3}$, and the parameter a_0 is excluded from consideration.

Acoustic instability in an oscillatory-excited gas can occur at certain values of the parameters $\tau_\varrho = \partial \ln \tau / \partial \ln \varrho$, $\tau_T = \partial \ln \tau / \partial \ln T$ and the degree of disequilibrium of the medium S. Inasmuch as, in the model under consideration (4) $\tau_\varrho = -1$, then the conditions under which sound waves are unstable are of the form [2,3,17]: $\tau_T < \gamma_1^{-1}$ and $S > \gamma_1 C_v (1 - \gamma_1 \tau_T)^{-1}$, where $\gamma_1 = \gamma - 1$, $C_v = R^{-1} \partial \varepsilon_v^e / \partial T$. Thus, the initial distribution of the parameters of the gas medium and the intensity of heating must satisfy these conditions, which provide the possibility of increasing the amplitude of acoustic waves at the initial linear stage of evolution according to the law $\propto \exp(\bar{\alpha} \bar{x})$, where $\bar{\alpha} = \alpha c_{s0} \tau_0$ — is a dimensionless acoustic increment. The maximum acoustic increment value is reached at $\bar{\omega} = \omega \tau_0 \approx 2\pi$ and is defined as $\bar{\alpha}_{\max} \approx \gamma_1 [S(1 - \gamma_1 \tau_T) - \gamma_1 C_v] / (2\gamma)$ [2,3].

Numerical experiments were conducted for different perturbation frequencies $\bar{\omega} = (0.5, 1, 2)\pi$. The computational domain $\bar{x} \in [0, \mathscr{L}]$ ($\mathscr{L} = 100$) was covered by cells of size $h = \mathscr{L}/N$, and the number of computational cells was specified within $N = 10^3 - 10^4$. The source of the stimulated disturbances localized at the origin ($|\bar{x}| < \bar{\lambda}/4$) is given as $\bar{g}(\bar{x}, \bar{t}) = \hat{g} \sin(\bar{\omega} \bar{t})$, where $\bar{\lambda} = 2\pi / \bar{\omega}$ — is the dimensionless wavelength of the perturbations, $\hat{g} \approx 10^{-4}$ — is the amplitude of the perturbing specific force. In as boundary conditions in numerical experiments, we will use the „rigid wall" condition on the left boundary, and on right — „the free flow condition". To demonstrate the main stages of the evolution of acoustic instability, the following basic parameters of the numerical model were chosen: $\gamma = 1.4$, $\bar{a}_1 = 10$, $\bar{a}_2 = \bar{a}_3 = n = m = 0$,
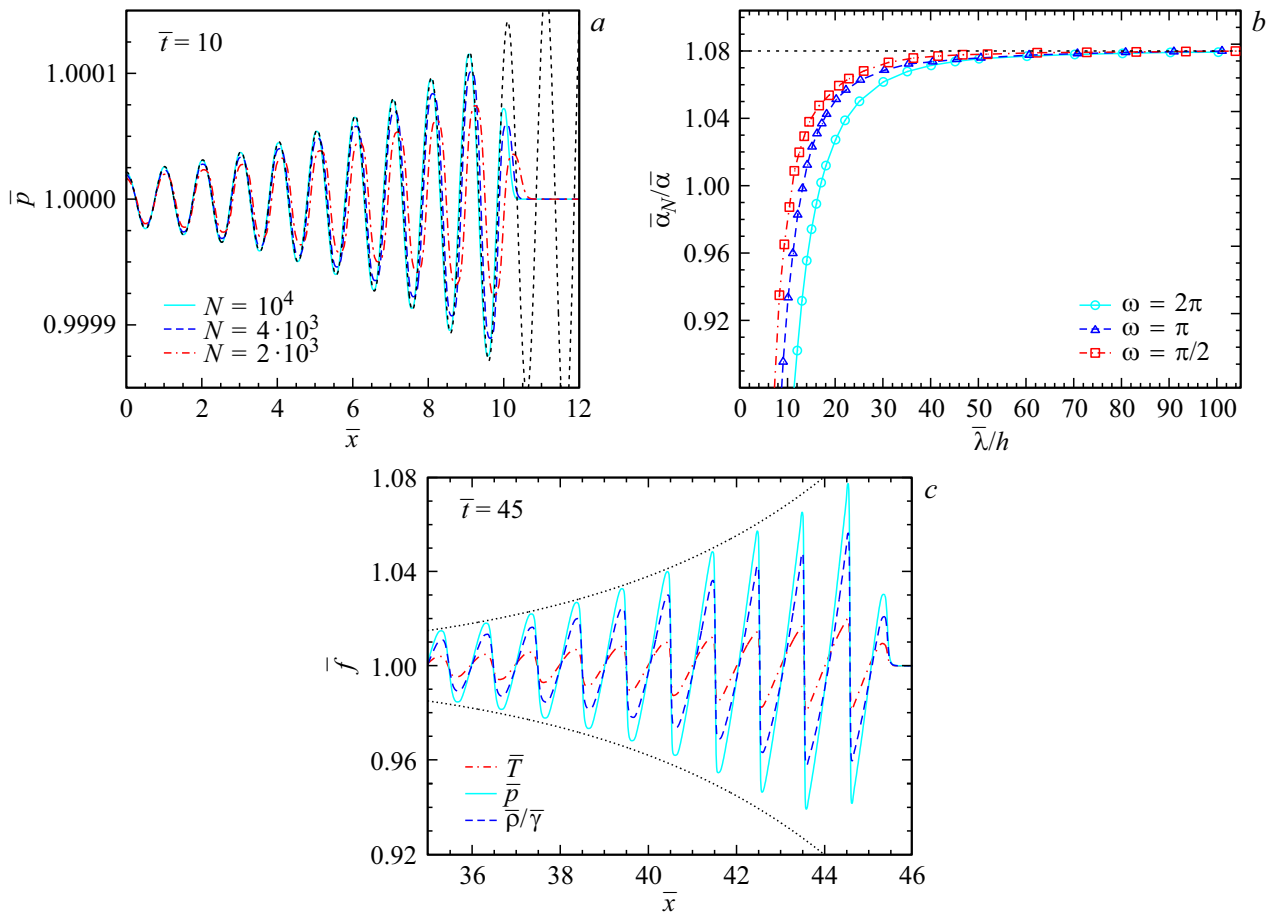
Figure 1. A Quasilinear Stage in the Evolution of Unstable Sound Waves. *a* — pressure distribution in an acoustic wave on condensing grids (linear stage); *b* — relationship of $\bar{\alpha}_N/\bar{\alpha}$ on spatial resolution $\bar{\lambda}/h$ for different frequency values $\bar{\omega}$; *c* — distribution of pressure, density, and temperature during the transient (quasi-linear) stage. The dotted line corresponds to the solutions of the linear model.

$\bar{\theta} = \bar{\theta}_\star = 6$, $\bar{\omega} = 2\pi$, $N = 10^4$. These baselines are further applied by default.

The quasilinear stage of the evolution of unstable acoustic waves is shown in Fig. 1. By the time $\bar{t} = 10$ (Fig. 1, *a*), the source generates a wave packet with ten maxima and an initial amplitude of relative pressure and density perturbations $\sim 10^{-5}$. As can be seen from Fig. 1, *a*, the generated wave packet is a harmonic wave with an exponentially increasing amplitude, with the exception of only the first maximum, which borders on an unperturbed medium and is the front (right) edge of the wave packet. For comparison with linear stability analysis [2,3], this figure presents the results of simulations on a sequence of condensing meshes, demonstrating the convergence of the numerical solution to the solution of the linear model: $\widetilde{f} = \widehat{f}_0 \exp(\bar{\alpha}\bar{x}) \sin(\bar{k}\bar{x})$, where $\widehat{f}_0$ — is the initial amplitude of the perturbations, $\bar{k}$ — dimensionless wavenumber. An important characteristic in simulation of the dynamics of unstable sound waves that affect the growth rate of perturbations in a numerical experiment is the spatial wave resolution, i.e., the number of cells per wavelength ($\bar{\lambda}/h$). Fig. 1, *b* for different frequencies shows the dependence on $\bar{\lambda}/h$ of the value of the acoustic increment $\bar{\alpha}_N$ obtained in

a numerical experiment with respect to $\bar{\alpha}$ from the linear model. It can be seen that at the values $\bar{\lambda}/h > 50$, the differences in the wave amplitude growth rate in the linear and numerical models are less than 1%. The evolution of unstable acoustic waves at the time $\bar{t} = 45$ (Fig. 1, *c*) can be characterized as a transitional stage from the linear to the nonlinear regime, in which the nonlinear winding of the wave fronts occurs and the linear sinusoidal profile is deformed into a nonlinear „sawtooth".

The nonlinear stage of acoustic instability evolution is shown in Fig. (2). By the moment of time $\bar{t} = 60$ (Fig. 2, *a*) there is a nonlinear saturation of the relative amplitude of perturbations at the level of $\sim 2.5-10\%$ ($\bar{f}_{max} \sim 1.025-1.1$), and the entire wave packet acquires „sawtooth" shape. At this stage, the unstable sound waves form a small-scale shock wave (SW) system with almost the same amplitude and spatial scale (distance between the fronts) $\sim \bar{\lambda}$. As can be seen from Fig. 2, *a*, at the boundary of the wave packet, the amplitude of the shock waves begins to change due to nonlinear interaction with neighboring shock waves within the wave packet and the undisturbed gas. The amplitude and velocity of the first maximum increase, which leads to the expansion of the
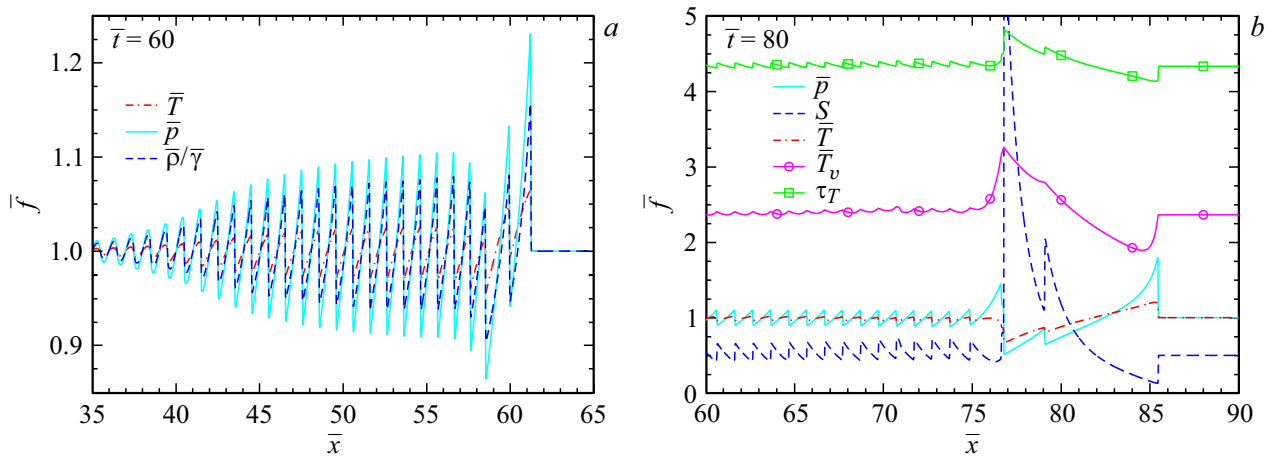
Figure 2. A nonlinear stage in the evolution of unstable sound waves. The spatial distributions of dimensionless parameters $\bar{f}$ in an acoustic wave at different time points are shown.
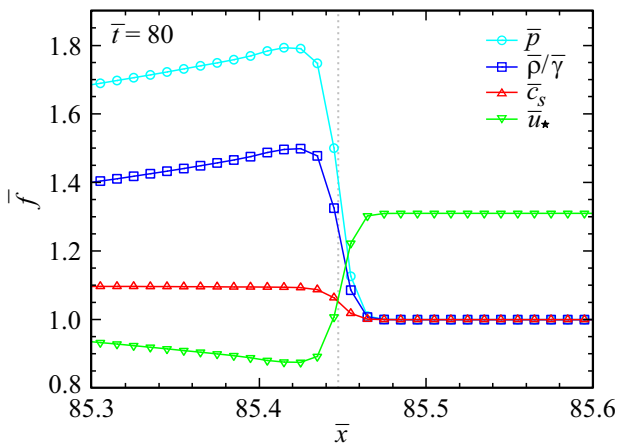

Figure 3. The SW structure in the region of the first maximum of the wave packet at time $\bar{t} = 80$ (see Fig. 2, b), where $\bar{u}_\star = |\bar{u} - \bar{u}_1|$ — is the velocity of gas flow to the front SW, $\bar{u}_1$ — SW velocity (of the first maximum of the wave packet).

wave packet. From Fig. 2, b it can be seen that with the further propagation of the SW system in space, the nonlinear effects of the expansion of the wave packet and the interaction of neighboring shock waves intensify. By time $\bar{t} = 80$, the pressure on the leading edge of the wave packet (first maximum) increases to $\bar{f}_{\max} \approx 1.8$, and the distance between the first and second maxima increases approximately 6.5 fold. At this stage of evolution between the first and third maxima, an area of low pressure and temperature is formed, with a minimum in the vicinity of the third maximum. As a result, the degree of nonequilibrium increases significantly ($S_{\max} > 5$), which leads to an additional nonlinear increase in instability and the disappearance of the nonlinear saturation effect in this field. Changes to other model parameters, such as τ_T and $\bar{T}_v$, also contribute to the effect of nonlinear instability amplification. A detailed study of these effects, including

the possible development of thermal instability in this field, is beyond the scope of this paper.

The structure of the shock wave formed at the time of time $\bar{t} = 80$ on the leading edge of the wave packet is shown in Fig. 3. The gas flows onto the right wave front at supersonic velocity $\bar{u}_\star = |\bar{u} - \bar{u}_1|$ (where $\bar{u}_1$ — SW velocity) and Mach number $\mathscr{M} = \bar{u}_\star / \bar{c}_s \approx 1.3$, and after passing through the sound point on the SW front, the flow becomes subsonic ($\mathscr{M} \approx 0.8$). The SW front in this numerical calculation is about 5 cells, which corresponds to $\sim 0.05\bar{\lambda}$. A similar structure of shock waves is formed in the vicinity of other maxima of the wave packet, but with smaller amplitudes of perturbations and deviations of the Mach number from unity ($\mathscr{M} \sim 1.08$).

Conclusions

On the basis of the numerical gas-dynamic method CSPH-TVD, a software package has been developed for the study of the nonlinear dynamics of acoustic instability in an oscillatory-excited gas with various relaxation models. The dynamics of unstable sound waves in nonequilibrium gas at the linear and nonlinear stages of acoustic instability development have been investigated. At the linear stage, the convergence of the numerical solutions of our model to the results of the linear stability analysis is shown. The nonlinear stage is characterized by the formation of a SW system with an almost constant amplitude for about ten maxima of the wave packet. In the vicinity of the leading edge of the wave packet, the effect of nonlinear instability amplification was detected, leading to rapid cooling of the gas and requiring more detailed further investigation with various models of oscillatory relaxation, heating, and cooling.

In this paper, numerical calculations are presented for the values of the parameters corresponding to the diatomic gas H_2 at the temperature $T_0 \approx 1000\,K$ and the pressure $p_0 = p_A$ [16]. The built numerical model can be used

to study the dynamics of acoustic instability in gases with several vibrational modes, for example, CO_2, having previously determined the total vibrational energy of the gas. In some approximation, our model can also be applied to gas mixtures, having previously calculated the average/effective values of the model parameters for the mixture, which will allow us to qualitatively determine the main regularities of the evolution of acoustic instability in such media, and then, if necessary, refine the solutions in the scope of a more complex multicomponent model.

Funding

Conflict of interest

The authors declare that they have no conflict of interest.

References

[1] A.I. Osipov, A.V. Uvarov. UFN, **162** (11), 1 (1992). DOI: 10.3367/UFNr.0162.199211a.0001

[2] V.G. Makaryan, N.E. Molevich. Fiziko-Khimicheskaya kinetika v gazovoy dinamike, **3**, id. 84 (2005). (In Russian). http://chemphys.edu.ru/issues/2005-3/articles/84/

[3] V.G. Makaryan, N.E. Molevich. Plasma Sources Sci. Technol., **16** (1), 124 (2007). DOI: 10.1088/0963-0252/16/1/017

[4] D. Zavershinskii, N. Molevich, S. Belov, D. Riashchikov, AIP Conf. Proc., **2304** (1), id. 020028 (2020). DOI: 10.1063/5.0034849

[5] T.G. Elizarova, A.A. Zlotnik, M.A. Istomina. AZh, **95** (1), 11 (2018). (In Russian). DOI: 10.7868/S0004629918010012

[6] M.A. Butenko, I.V. Belikova, N.M. Kuzmin, S.S. Khokhlova, G.S. Ivanchenko, A.V. Ten, I.V. Kudina. Matemat. Fizika i komp. modelirovanie, **25** (3), 73 (2022) (in Russian). DOI: 10.15688/mpcm.jvolsu.2022.3.5

[7] G.V. Shoev, E.A. Bondar, G.P. Oblapenko, E.V. Kustova. Teplofizika i aeromekhanika, **23**, (2), 159 (2016) (in Russian).

[8] A.V. Khoperskov, S.S. Khrapov, E.A. Nedugova. Astronomy Lett., **29** (4), 246 (2003). doi.org/10.1134/1.1564856

[9] L. Landau, E. Teller. Phys. Z. Sowjetunion, **10**, 34−43 (1936).

[10] A.A. Kosareva, E.A. Nagnibeda. Vestnik of SPbGU, Ser. 1, **3** (61), 468–2016 (2014). (in Russian).

[11] R.C. Millikan, D.R. White. J. Chem. Phys., **39**, 3209 (1963).

[12] E.V. Kustova, G.P. Oblapenko, I.Z. Sharafutdinov. Fiziko-Khimicheskaya kinetika v gazovoy dinamike, **16**, id. 536 (2015). (In Russian).http://chemphys.edu.ru/issues/2015-16-2/articles/536/

[13] B.F. Gordiets, A.I. Osipov, E.V. Stupochenko, L.A. Shelepin. UFN, **108** (4), 655 (1972).

[14] C. Park. *Nonequilibrium Hypersonic Aerothermodynamics.* (J. Wiley and Sons, NY., Chichester, Brisbane, Toronto, Singapore, 1990).

[15] E.A. Kovach, S.A. Losev, A.L. Sergievskaya, N.A. Khrapak. Fiziko-khimicheskaya kinetika v gazovoy dinamike, **10**, id. 332 (2010). (in Russian). http://chemphys.edu.ru/issues/2010-10/articles/332/

[16] V.E. Alemasov, A.F. Dregalin, A.P. Tishin, V.A. Khudyakov, V.N. Kostin. *Thermodinamicheskie i teplofizicheskie svoistva produktov sgoraniya,* (VINITI, AN USSR, M. 1980), v. 10, № 1, 379 p. (in Russian).

[17] S. Khrapov, A. Khoperskov. J. Conference Series, **973**, 012007 (2018). DOI: 10.1088/1742-6596/973/1/012007

[18] S. Khrapov, A. Khoperskov, S. Khoperskov. J. Conference Series, **1392**, 012041 (2019). DOI: 10.1088/1742-6596/1392/1/012041

Translated by 123